Functional switch between motor tracts in the presence of the mAb IN-1 in the adult rat

Olivier Raineteau*, Karim Fouad, Pascal Noth, Michaela Thallmair, and Martin E. Schwab

Brain Research Institute, University and Swiss Federal Institute of Technology (ETH) Zurich, Winterthurerstrasse 190, 8057 Zurich, Switzerland

Communicated by Hans Thoenen, Max Planck Institute of Neurobiology, Martinsried, Germany, April 3, 2001 (received for review February 19, 2001)

Fine finger and hand movements in humans, monkeys, and rats are under the direct control of the corticospinal tract (CST). CST lesions lead to severe, long-term deficits of precision movements. We transected completely both CSTs in adult rats and treated the animals for 2 weeks with an antibody that neutralized the central nervous system neurite growth inhibitory protein Nogo-A (mAb IN-1). Anatomical studies of the rubrospinal tracts showed that the number of collaterals innervating the cervical spinal cord doubled in the mAb IN-1- but not in the control antibody-treated animals. Precision movements of the forelimb and fingers were severely impaired in the controls, but almost completely recovered in the mAb IN-1-treated rats. Low threshold microstimulation of the motor cortex induced a rapid forelimb electromyography response that was mediated by the red nucleus in the mAb IN-1 animals but not in the controls. These findings demonstrate an unexpectedly high capacity of the adult central nervous system motor system to sprout and reorganize in a targeted and functionally meaningful way.

In the case of incomplete injuries of the central nervous system (CNS), spontaneous recovery processes can be observed in humans (1, 2) as well as in different animal models (3, 4). However, in the adult mammalian CNS, this recovery remains largely incomplete. This inability of the CNS to fully recover from an incomplete lesion appears gradually during development at a time coincident with the appearance of myelin (5, 6). Several myelin-associated proteins and proteoglycans show inhibitory properties to neurite growth; among them are Nogo-A/NI-250 (7, 8), myelin-associated glycoprotein (9, 10), tenascin-R (J1 160/180; janusin) (11), and sulfated proteoglycans (12, 13). The inhibitory effect of these proteins can be overcome in different ways: e.g., by a direct masking of the inhibitory substrate. Neutralization of Nogo-A by mAb IN-1 leads to a large decrease in the inhibitory activity of oligodendrocytes and myelin *in vitro* (14, 15) as well as *in vivo*, resulting in long-distance regeneration of lesioned spinal cord (16).

Recent experiments have also pointed to a role of Nogo-A in inhibiting the plastic reorganization of the lesioned adult CNS. Infusion of the Nogo-A-neutralizing mAb IN-1 into the cerebrospinal fluid of unilaterally pyramidotomized rats induced corticorubral and corticopontine fibers to sprout across the midline and establish bilateral, anatomically specific projections (17). At spinal cord level, the unlesioned corticospinal tract (CST) sprouted into the contralateral denervated spinal cord (18). These anatomical changes were associated with an almost complete functional recovery in different behavioral tasks. These studies, however, focused on the CST, i.e., the lesioned system, and raised the interesting question of the limits of such repair processes. Thus, after complete transection of the CST, other descending motor tracts may also undergo reorganization and thereby contribute to the functional recovery. The rubrospinal tract (RST) is of particular interest in the study of such compensatory mechanisms. The RST and the CST originate from the red nuclei and sensorimotor cortex, respectively. Both areas are somatotopically organized, with a greater representation of distal than of proximal limbs (19). Both systems show a similar pattern of discharges during reaching and grasping movements (20, 21), suggesting that both tracts cooperate in producing skilled movements. Particular evidence for cooperation between the two tracts comes from lesion studies. With rats, detailed behavioral observations have revealed additional effects of a red nucleus lesion subsequent to a pyramidotomy (22). Experiments performed with monkeys suggest that one system can compensate functionally after a lesion of the other: monkeys subjected to a unilateral pyramidotomy partially recovered voluntary control of arm and foot. This incomplete recovery disappeared, however, when the red nucleus innervating the affected side was subsequently lesioned (23).

The purpose of the present study was to investigate the anatomical reorganization of the RST in response to a selective, complete removal of the CST and the subsequent neutralization of the myelin-associated inhibitor Nogo-A in the rat. Our results show an increased innervation of the cervical spinal cord by the RST after bilateral pyramidotomy (bPT) and subsequent treatment with mAb IN-1. Electrophysiological and behavioral experiments indicate that these anatomical changes are functionally meaningful.

NEUROBIOLOGY

Materials and Methods

Adult Lewis rats of both sexes ($n = 61$) and of a mean age of 2.5 months (body weight = 226 ± 54 g) were used in this study. The animals were divided into four experimental groups: unlesioned (Unles., $n = 12$); animals that underwent only bPT (bPT, $n = 7$); bPT animals treated with a control antibody against horseradish peroxidase (anti-HRP) (bPT + anti-HRP, $n = 19$); and animals with bPT and treatment with mAb IN-1 neutralizing the myelin-associated neurite growth inhibitor Nogo-A (bPT + mAb IN-1, $n = 23$) (7, 14). The experiments were approved by the Veterinary Department of the Canton of Zurich.

Pyramidotomy and Antibody Application. Rats were anesthetized by using a combination of Hypnorm (0.3 mg/kg, i.p.) and Dormicum (0.6 mg/kg, i.p.) (Roche, Basel, Switzerland). A bilateral lesion of the CST at the level of the medulla oblongata was performed by using a ventral approach (18). For constant antibody supply, ≈10^5 living hybridoma cells were stereotaxically implanted into the left hippocampal formation (4 mm caudal, 5 mm lateral to bregma, depth = 5 mm). This location was chosen to avoid damage to motor systems by the injection or by growth of the cells and to allow antibody diffusion into the ventricular system. At 1 day before hybridoma cell implantation and during the following 6 days, all animals received a daily i.p. injection of cyclosporin A (Sandimmun, 10 mg/kg of body weight, i.p.; Novartis, Basel, Switzerland). After surgery, all animals were kept on a heating plate (at 38°C) until fully awake and all

Abbreviations: CNS, central nervous system; CST, corticospinal tract; RST, rubrospinal tract; BDA, biotin dextran amine; bPT, bilateral pyramidotomy; anti-HRP, anti-horseradish peroxidase; EMG, electromyography; ICMS, intracortical microstimulation.

*To whom reprint requests should be addressed: E-mail: rainet@hifo.unizh.ch.

The publication costs of this article were defrayed in part by page charge payment. This article must therefore be hereby marked "*advertisement*" in accordance with 18 U.S.C. §1734 solely to indicate this fact.

received Rimadyl, a pain killer (carprofen, 5 mg/kg of body weight, i.m.; Pfizer, Karlsruhe, Germany), for 2 days.

Tracing of the Rubrospinal Tract. Iontophoretic injections (1 μA; 7 sec on/off; 15 min) of a 10% (wt/vol) solution of biotinylated dextran amine (BDA, 10,000 molecular weight; Molecular Probes) in 0.01 M phosphate buffer (pH 7.4) were made into the right red nucleus (4.9 mm posterior to bregma, 1.4 mm lateral, 7.8 mm ventral to the skull surface).

Fourteen days after tracer injection, the animals were deeply anesthetized with pentobarbital (Nembutal, 450 mg/kg, i.p.; Abbott) and perfused through the left ventricle with Ringer's solution containing 100,000 units/liter heparin (Liquemin; Roche, Basel, Switzerland) and 0.25% $NaNO_2$ followed by 4% (vol/vol) paraformaldehyde in 0.1 M phosphate buffer with 5% (wt/vol) sucrose. The brains and spinal cords were dissected and postfixed overnight at 4°C in the same fixative. Sections of the cervical spinal cord (50 μm) were cut in the horizontal plane (segments C_1 to C_5) and in the frontal plane (segment C_6) and checked for BDA by using a nickel-enhanced diaminobenzidine protocol (Sigma), according to the semifree floating technique (24). The sections were air dried, lightly counterstained with cresyl violet, and coverslipped.

Quantification of the Anatomical Reorganization. The number of collaterals emerging from the RST was analyzed on horizontal sections of the rostral cervical spinal cord (C_1 to C_5) by counting the intersections of BDA-labeled fibers with a rostrocaudal line positioned at the white matter–gray matter (dorso-lateral funiculus–dorsal horn) interface (Fig. 1*A*).

Sprouts were quantified on every section of the series. The sum of the collaterals was normalized for interindividual tracing variability as follows. (*i*) The number of BDA-positive RST fibers was determined on three randomly chosen spinal cord cross sections at the C_6 level. The number of collaterals was divided by the number of labeled RST fibers for each animal. (*ii*) Because of the somatotopic organization of the red nucleus and small variations of the BDA injection sites, different proportions of RST fibers projecting to the cervical vs. more caudal segments were labeled. To correct for this result, the ratio of labeled RST fibers at C_1 vs. C_6 was determined. The value obtained under *i* was divided by this ratio for each rat. (*iii*) Finally, the total length of the spinal cord on which the counting was performed was measured to express the result as a percentage of RST fiber per mm (one RST axon can give rise to more than one collateral).

Behavioral Testing. *Food pellet-reaching task.* During the entire behavioral testing period, the rats from the different treatment groups were number-coded, randomly mixed, and grouped as four or five individuals per cage. They were kept in a 12-h light/12-h dark cycle. Animals had full access to water but were food-deprived to ≈90% of their original body weight during the entire experimental period. Food was given after the testing sessions.

Before the surgery, all animals were trained daily at a fixed time of the day, until their performance reached a plateau for 3 successive days. The baseline measurements were video recorded (50 frames per sec) and the animals were divided into two comparable groups. All rats underwent a bPT, and hybridoma cells secreting the IN-1 antibody ($n = 11$) or a control anti-HRP antibody ($n = 10$) were transplanted into the left hippocampal region as described above. No tracing was performed in these animals. Postoperative testing was then performed every 3 to 4 days for 4 weeks. Video recordings were performed on days 14 and 25 postoperatively.

The following test was performed as described (17) by using a transparent Plexiglas chamber (30 × 36 × 30 cm) but with a rectangular opening (1.5 × 2 cm) in the middle of the front wall.

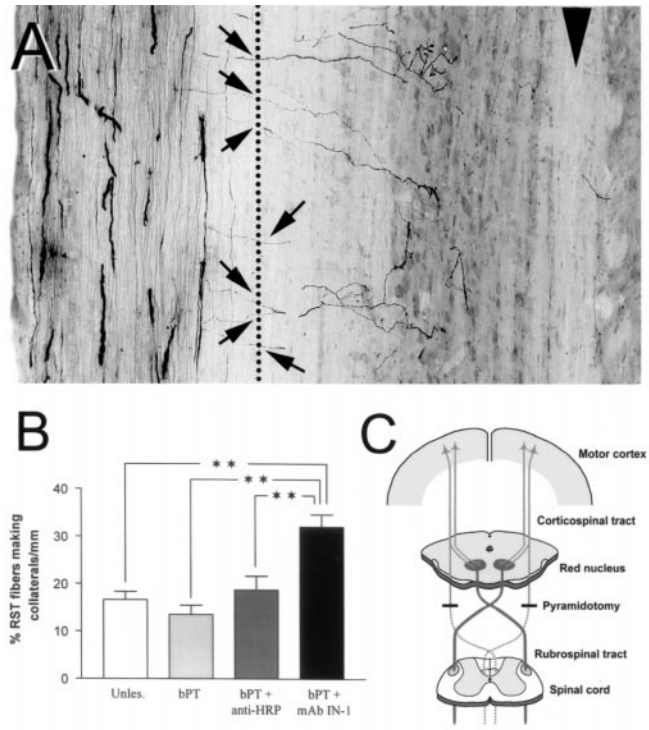

Fig. 1. RST collateral formation after bPT. (*A*) Photomicrograph of a horizontal section of the rostral cervical spinal cord of a rat in which both CSTs have been transected and the RST traced. Descending RST fibers in the dorsolateral funiculus make collaterals (arrows) projecting to the gray matter where they arborize. Arrowhead indicates the midline. To measure the amount of collaterals emerging from the RST, all fibers crossing a line positioned 450 μm from the section border were counted and normalized as described in *Materials and Methods*. (*B*) Quantitative analysis showing the percentage of RST fibers making a collateral on a length of spinal cord of 1 mm. Unles, unlesioned rats, $n = 6$; bPT, lesioned rats, $n = 7$; bPT + anti-HRP, lesioned rats treated with the control antibody anti-HRP, $n = 9$; bPT + mAb IN-1, lesioned rats treated with the mAb IN-1, $n = 12$. **, $P < 0.01$. (Bars = +SEM.) (*C*) Scheme of the cortico- and rubrospinal projections and the lesion sites.

Before the bPT, the rats were individually trained to pull sucrose food pellets (45 mg; Bilaney Consultants, Frenchtown, NJ) through the opening by using their preferred limb. Three parameters were measured: (*i*) the amount of time needed to grasp 10 pellets (i.e., time rate); (*ii*) the total number of pellets grasped and eaten (i.e., success rate); and (*iii*) the maximum number of attempts to grasp a pellet successfully.

Video analysis of movement components. Qualitative analysis of video recordings was performed by attributing a "disability score" to different movement parameters, as described (17). The nine parameters analyzed were movement initiation, aim, advance, digits open, pronation, grasp, supination, food release, and movement stop.

Each of these movements was rated on a four-point scale: 0 was given for normal movements in >90% of the observations; 1 was given for movements that appeared slightly abnormal in <50% of the observations; 2 was given for abnormal movements in >50% of the observations; and 3 was given for no movements or if other parts of the body compensated for movements.

Statistical analysis of the behavioral data was performed with GRAPHPAD PRISM 2.01. For comparison between the same experimental units, i.e., between baseline and postoperative testing, a Wilcoxon signed-rank test was used; for testing between different experimental units, i.e., between two groups of animals, a Mann–Whitney *U* test was used. All data are presented as means ± SEM.

Electrophysiology. Unlesioned rats ($n = 6$) as well as the 21 behaviorally tested rats underwent microstimulation of the sensorimotor cortex and of the red nucleus on both sides. Electromyographic (EMG) recordings of a group of medial muscles (i.e., extensor carpi radialis and extensor digitorum communis) from both forelimbs were performed to quantify the evoked movements and the latency of their responses.

The animals were anesthetized with ketamine (500 mg/kg of body weight, i.p.; Chassot, Bern, Switzerland) and secured in a stereotaxic frame. A customized tungsten microelectrode was inserted in three to eight points of the forelimb area (25) of the primary motor cortex of both hemispheres at depths of 1.5–1.9 mm. The microelectrode was then placed in both red nuclei by using the coordinates above. The stimulation consisted of a train of cathodal pulses ($n = 30$, 0.25 msec, 330 Hz). For EMG recordings, two pairs of multistranded Teflon-coated wires (Cooner Wire, Chatsworth, CA) with exposed tips of about 2 mm were inserted as electrodes into the forearm extensors of both forelimbs. The EMGs were amplified (Cyber-Amp; Axon Instruments, Foster City, CA), digitized (sampling rate = 5 kHz), and filtered (30–300 Hz) with the Digi-Data interface (Axon Instruments). The electrode position and the type of movement were noted for every stimulation in which the lowest stimulation threshold evoked a muscle response. The delay of the EMG response was measured with the AXOSCOPE program (Axon Instruments) from the first stimulus pulse to the onset of EMG activity (after summation of 25 to 35 EMG traces). Whenever the intracortical microstimulation (ICMS) elicited EMG activity in the lesioned animals, both red nuclei were transiently hyperpolarized by injecting stereotactically 0.8 μl of the γ-aminobutyric acid agonist muscimol (1 μg/μl in 0.9% saline). Both the localization of the red nucleus stimulation and of the muscimol injection sites were confirmed by histological examinations.

Results

Anatomical Reorganization of the RST. The RST originates from the caudal part of the red nucleus (i.e., the magnocellular part), located in the ventral part of the midbrain (Fig. 1*C*). Because of the presence of numerous other spinal-projecting nuclei in this region (e.g., interstitial nucleus of Cajal and the reticular formation of the midbrain), very local, small tracer injections were performed. Typical iontophoretic injection sites had diameters of 200 to 400 μm with no signs of necrosis; they resulted in an intense staining of 100–200 RST fibers of large and small diameters.

Both CSTs were transected completely with little damage to the underlying rostral olivary complex or to other deeper structures (bPT; Fig. 1*C*). The RST runs ≈1.5 mm lateral to the pyramidal tract, and was untouched by the pyramidotomy. Lesion completeness was carefully assessed under a binocular microscope and in a sample of animals by tracing of the CST. Animals with incomplete lesions (7 of 61) were excluded from the study.

Hybridoma cells were transplanted close to the lateral ventricle, into which they released important quantities of antibodies. Immunostaining experiments performed after cell implantation or intraventricular infusion by using osmotic minipumps revealed an intense staining of the ventricles and of the surface of the brain and spinal cord. Gradients of immunoreactivity could be detected in the parenchyma of the brain and spinal cord (ref. 17; O. Weinmann and M.E.S., unpublished observations).

Being involved in forelimb movement control, the RST showed frequent collaterals branching into the cervical spinal cord gray matter (Fig. 1*A*). In normal, unlesioned animals, 16.6% ± 1.7% ($n = 6$) of the RST fibers project to the gray matter on a spinal cord length of 1 mm, as quantified by counting intersections of the RST collaterals with a rostrocaudal line positioned at the white matter–gray matter (dorsolateral funiculus–dorsal horn) interface. This value was comparable to that of the lesion-only group (13.5% ± 2%, $n = 7$) as well as that of the lesioned, anti-HRP-treated animals (18.7% ± 2.9%, $n = 9$). However, after lesion and treatment with the mAb IN-1, a significant, 2-fold increase in the number of collaterals emerging from the RST could be observed (32% ± 2.6%, $n = 12$; Fig. 1*B*). Most of these collaterals terminated in the normal RST target area (intermediate layers of the spinal cord). Interestingly, however, some fibers in the mAb IN-1 animals extended to the deep ventral horn, where they contacted motoneurons (O.R., K. F., and M.E.S., unpublished data).

Behavioral Recovery. To investigate whether the observed anatomical reorganization of the RST after a bPT and subsequent neutralization of the myelin-associated inhibitory protein Nogo-A resulted in a functional recovery, the rats were tested in a forelimb reaching task (ref. 26; Fig. 2*A*). The rats were trained daily for 3 weeks before any experimental intervention. After having reached a stable baseline for 3 consecutive days, the animals were randomly assigned to two experimental groups, coded to make the experimenter blind to the treatment, and mixed in the cages. Both groups showed similar preoperative scores in all the forelimb grasping tasks—time to grasp 10 pellets, success rate, and maximum number of attempts to grasp ($P > 0.5$). After surgery and hybridoma cell implantation, the animals were tested every 3 to 4 days for a period of 4 weeks.

The first analysis performed consisted in measuring the time the rats needed to grasp and eat 10 stabilized food pellets. Before surgery, all animals performed this task in 39.5 ± 3.5 sec. At 3 days after bPT (i.e., the first time-point analyzed), both groups showed strong impairments, requiring more than 90 sec to perform the task. Both groups then showed recovery that reached a plateau 10 days after operation. At this time, lesioned mAb IN-1-treated rats approached baseline values, whereas the lesioned anti-HRP-treated animals showed a marked and persistent deficit, performing the task in 53.8 ± 3 sec on day 25. The difference between the two experimental groups was significant at days 10, 17, 20, and 25, the latest time-points analyzed (Fig. 2*B*).

A similar outcome was observed for the success rate and the maximum number of attempts. Before the operation, the animals successfully grasped an average of 8.8 ± 0.15 ($n = 21$) pellets of the 10 presented and made a maximum number of attempts of 1.9 ± 0.12 ($n = 21$). Both animal groups showed marked deficits in both parameters 3 days after bPT. As soon as 7 days after lesion and for the rest of the testing period, the lesioned IN-1-treated rats recovered to the baseline levels, whereas the lesioned anti-HRP-treated animals presented marked deficits, reaching only 6.6 ± 0.3 sucrose pellets of 10 and making a maximum of 3 ± 0.2 attempts to grasp on day 25 (Fig. 2 *C* and *D*).

To assess whether the functional recovery observed in the mAb IN-1-treated animals resulted from the development of new movement strategies or from the recovery of normal reaching movements, video recordings of the entire testing session were performed at days 14 and 25 after operation and were compared with preoperative recordings. The nine specific movement components of the grasping movement were analyzed by using the four-point disability score system described elsewhere (ref. 26; see also *Materials and Methods*). The ratings obtained at 14 and 25 days after operation were identical and are shown in Fig. 3. Lesioned anti-HRP-treated rats manifested a hesitation or even a complete inability of movement initiation. Persistent impairments of aiming, advance, pronation, grasp, supination, and food release were observed. In the aiming and advance component, these animals revealed ataxia and showed a reduced extension of the forelimb. Very much in contrast, mAb IN-1-treated rats showed a large, sometimes complete recovery in movement initiation, aim, advance, digit opening, pronation,

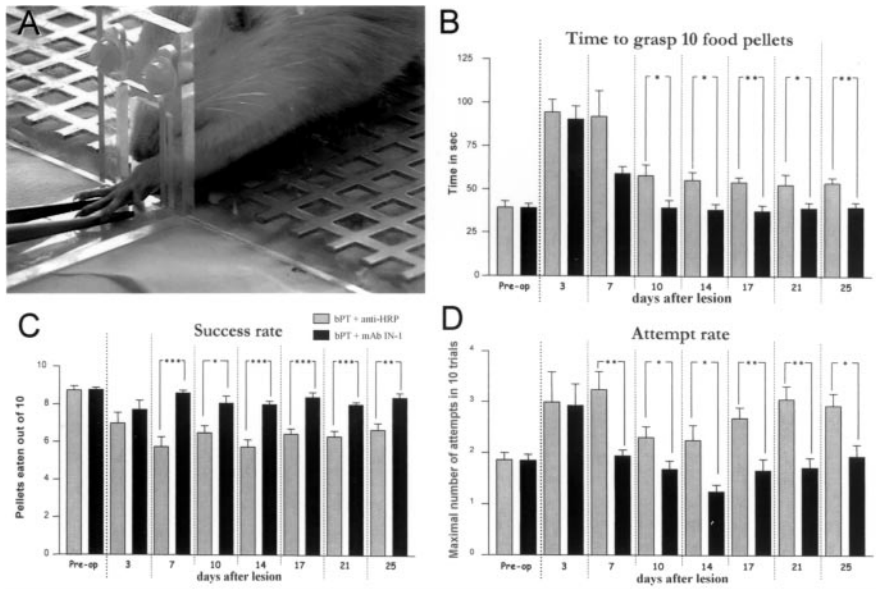

Fig. 2. Food pellet-reaching task. (*A*) Rat grasping small food pellets stabilized with a forceps through a central opening in the wall of a transparent Plexiglas box. (*B–D*) Time course of recovery for the time (in sec) needed to grasp 10 pellets (*B*), the success rate in grasping 10 pellets (n = number of pellets grasped and eaten) (*C*), and the maximum number of attempts (n) to grasp a pellet in 10 trials (*D*). *, $P < 0.05$; **, $P < 0.01$; ***, $P < 0.001$. (Bars = +SEM.)

grasp, and food release as soon as 14 days after lesion (i.e., the first time-point of video recording). A partial although reduced impairment in comparison to the lesioned anti-HRP-treated animals was still present for paw supination and pronation (Fig. 3).

The sum of all movement component scores obtained in the two experimental groups is presented as a combined movement score (not shown). At day 14 and 25, the disability score of the lesioned anti-HRP-treated animals was significantly higher than the preoperative baseline values ($P < 0.008$). In contrast, mAb IN-1-treated, lesioned animals showed a major and significant improvement ($P < 0.001$) but failed to reach baseline levels ($P = 0.04$). These results indicate that the functional recovery observed in the 10 pellets-reaching-paradigm in the mAb IN-1-treated group cannot be attributed to development of new strategies but rather is the result of a recovery of a normal movement.

Electrophysiological Results. To investigate the role of the reorganization of the cortico-rubro-spinal circuitry in the observed functional recovery, electrophysiological experiments were performed. EMG activities of the medial forelimb muscles extensor and flexor digitorum were analyzed after intracortical as well as red nuclei microstimulations.

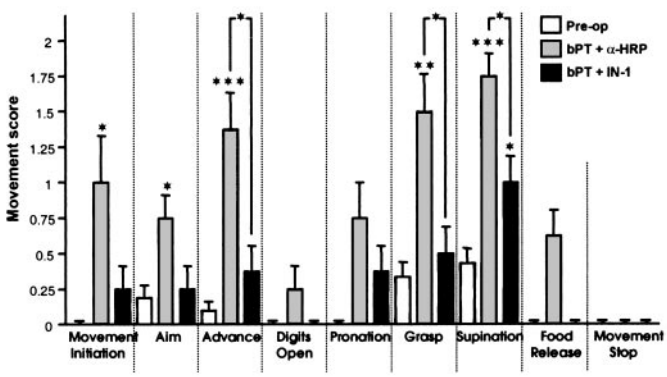

Fig. 3. Video analysis of movement components. Individual movement components on day 14 after operation. A score of 0 indicates normal forelimb performance; 3 indicates an absence of movements. Asterisks on top of error bars indicate significance compared with preoperative values; asterisks on the very top indicate a comparison between the two experimental groups. *, $P < 0.05$; **, $P < 0.01$; ***, $P < 0.001$. (Bars = +SEM.)

Electrophysiological properties of the RST. To investigate the electrophysiological consequences of the observed anatomical reorganization of the RST after complete CST removal and antibody treatment, direct stimulations of the red nuclei with simultaneous EMG recordings of the medial muscles of both forelimbs were performed. In both unlesioned and lesioned anti-HRP-treated animals, minimal stimulation intensities of 19.1 ± 1.2 μA (n = 12) and 18.7 ± 0.6 μA (n = 18), respectively, were sufficient to obtain an EMG response in the contralateral medial muscles (i.e., extensor carpi radialis and extensor digitorum communis). This threshold intensity was significantly reduced to 14.6 ± 0.5 μA in the lesioned mAb IN-1-treated rats (Fig. 4*A*).

Reconnection of the sensory-motor cortex to the periphery through the red nucleus. In all anesthetized, unlesioned animals, focal stimulation of the forelimb area of the motor cortex at an intensity of 50 μA resulted in a consistent movement of the contralateral forelimb. Averages of 25 to 35 stimulation recordings showed a quick EMG response with a mean latency of 13.4 ± 0.8 msec (n = 10) in the medial muscles of the contralateral forelimb. When stimulation intensity was increased to 55–60 μA, an ipsilateral EMG activity with a longer onset latency (25.1 ± 2.5 msec) was recorded in 60% of the animals. After bPT and treatment with the control anti-HRP antibody, neither movements nor EMG responses could be elicited in both the ipsi- or contralateral forelimb at stimulation intensities up to 150 μA (n = 18). Interestingly, in 10 of 11 lesioned, IN-1-treated animals a movement could be elicited after low-intensity cortical stimulation. Of these 10 animals (20 hemicortices analyzed), six stimulations elicited a shoulder or trunk movement but no EMG activity in the recorded muscles of the forelimb; 10 stimulations led to a clear movement of the forelimb and to forelimb muscle EMGs. In these animals, the EMG latency in the contralateral medial forelimb muscle was slower than in normal animals (44.4 ± 9.7 msec). In only two cases could an ipsilateral EMG response be elicited that had a similar latency of 45.5 msec (Fig. 4*B*).

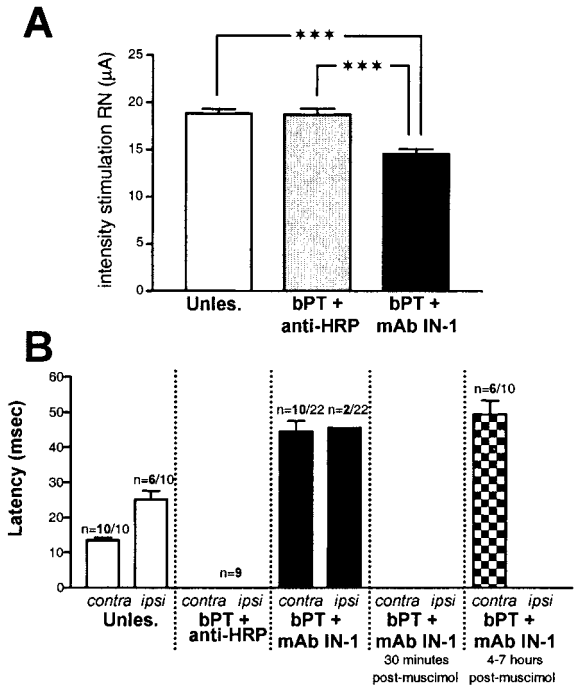

Fig. 4. Electrophysiological assessment of the cortico-rubro-spinal pathway reorganization. (*A*) Red nucleus thresholds of stimulation to obtain a peripheral EMG activity in the forearm muscles (extensor carpi radialis and extensor digitorum communis). Unles., unlesioned rats, $n = 5$; bPT + anti-HRP, lesioned rats treated with the control antibody against HRP, $n = 9$; bPT + IN-1: lesioned rats treated with the mAb IN-1, $n = 11$. ***, $p < 0.001$. (Bars, +SEM.) (*B*) EMG latencies for forearm muscles elicited by ICMS of the forelimb area in unlesioned, lesioned control-antibody (anti-HRP Ab), and lesioned, mAb IN-1-treated rats. ICMS in normal animals (5 rats, 2 hemicortex stimulations per rat) resulted in fast contralateral responses. An ipsilateral EMG response with a prolonged delay could also be found, but only at higher stimulation intensity. ICMS of the lesioned animals treated with the control antibody never resulted in movements ($n = 9$). In rats lesioned and treated with the mAb IN-1 ($n = 11$), ICMS led to contralateral EMG activity of increased latency. In two cases, an ipsilateral EMG response of comparable latency occurred. Muscimol injections into both red nuclei led to a loss of EMG activity. At 4–7 h after muscimol injection, ICMS resulted again in peripheral EMG activity. Unles., unlesioned rats; bPT + anti-HRP, lesioned rats treated with the control antibody against HRP; bPT + IN-1: lesioned rats treated with the mAb IN-1. (Bars, +SEM.)

To assess the possible role of the red nucleus in the observed reconnection of the sensorimotor cortex to the periphery, we infused 0.8 μl of a solution of the γ-aminobutyric acid receptor agonist muscimol (1 μg/μl) into each red nucleus of the rats in which forelimb EMG activity could be elicited. At 30 min after infusion, stimulation of the sensorimotor cortex at suprathreshold intensity (up to 150 μA) failed to elicit forelimb EMG responses in 9 of 10 lesioned, IN-1-treated animals. The peripheral EMG response could not be blocked by muscimol in only one of the anti-HRP-treated animals and one of the mAb IN-1-treated animals. These two animals had incomplete lesions as shown subsequently by the anatomical analysis of the lesion sites; they were removed from the study. After the muscimol injection (4–7 h), stimulation of six hemicortices again evoked movements and EMG responses (mean latency = 49.33 ± 4.05 msec; Fig. 4*B*).

Histological analysis of the red nuclei of all animals showed that all injections were centered within the nuclei and resulted in a small necrotic area.

Discussion

The present results show that sprouting from an intact descending tract in response to a complete transection of the CST can occur in the mature spinal cord in the presence of the mAb IN-1, which binds to and neutralizes the myelin-associated inhibitory protein Nogo-A (7). This sprouting response leads to a nearly complete recovery of fine arm and hand movements in which the cortico-rubro-spinal pathway plays a key role.

Anatomical Reorganization of the Rubrospinal Tract After bPT. After unilateral PT in adult rats combined with subsequent treatment with the mAb IN-1, but not after mAb treatment alone, sprouting of the corticospinal and corticobulbar system had previously been observed. These animals showed a high degree of functional recovery in a grasping task (17). The present study extends further these original observations by demonstrating that another important descending tract, the RST, is able to reorganize anatomically after CST lesion.

The present observations increase the body of evidence that, in addition to being involved in the inhibition of regeneration after CNS injury (16) by direct action on the growth cone of regrowing fibers (15), the protein Nogo-A might act as a general regulator of growth responsiveness in the adult mammal CNS (27, 28). Thus, by neutralizing the protein Nogo-A, the CNS is placed back in a developmental stage, and global anatomical reorganization can occur.

One important question concerns the mechanisms of induction of the new collaterals after Nogo-A neutralization. In development, axon shafts can respond to target-derived signals independently of the primary growth cone (29). The nature of these signals is still unclear, but diffusible factors such as neurotrophins (30) or slit-related proteins (31) may play a key role in this process. A similar mechanism may occur in our experiment. Branch-inducing and attractive factors may be up-regulated by CST target cells after denervation, as already shown in other systems (32, 33). Thus, neurotrophins have been shown to be rapidly up-regulated in the spinal cord in pathologic conditions, as, for example, by high glutamate, which is released in important quantities after spinal cord injury (34), as well as after dorsal rhizotomy in the cervical ventral spinal cord (35). The guidance of new collaterals to appropriate targets in the denervated spinal cord may also be of crucial importance for a functional recovery to occur. Indeed, in a parallel series of experiments, a high degree of specificity of spinal cord ventral horn reinnervation was observed (O.R., K.F., and M.E.S., unpublished data). Reexpression of guidance cues as well as activity-dependent refinement by stabilization or pruning of originally diffuse sprouts may collaborate to achieve targeting of sprouting RST fibers.

Functional Recovery. After partial lesions of specific parts of the CNS, spontaneous but often very limited recovery can be observed (3, 4). In the case of CST lesions, several lines of evidence point to a role of the RST in this spontaneous recovery. Thus, a lesion of the RST subsequent to a bPT in the monkey abolishes the observed partial recovery (23). Moreover, the red nucleus receives input from the motor cortex, and the CST and the RST have been shown to converge onto the same spinal interneurons in lamina V and VI (36, 37). The slow, restricted spontaneous recovery observed in the control groups may, therefore, also include a contribution of the RST.

In contrast to the very incomplete functional recovery in the control group, a nearly complete recovery of arm and hand movements during food pellet grasping was found in the mAb IN-1-treated animals. For all parameters analyzed, the mAb IN-1 animals recovered to their preoperative levels in 7 to 10 days. This time course points to a fast reorganization of the circuitry and correlates well with the expected time course of the mAb IN-1 availability in the rat CNS, the IN-1-secreting hybridoma cells being resorbed shortly after termination of the cyclosporin treatment (i.e., 6 days after operation). It is also consistent

with recent results obtained in the intact cerebellum where, after injection of mAb IN-1 or a new antibody against Nogo-A, numerous sprouts could be seen to emerge from Purkinje cell axons within 48 h (28).

Electrophysiological Evidences for Rewiring of the Lesioned Motor System. After bPT and subsequent mAb IN-1 treatment, electrophysiological analysis of the cortico-rubro-spinal system revealed several major changes. First, the motor cortex (which had lost its direct connection to the spinal cord) became reconnected to the periphery, as shown by the reappearance of EMG activity after cortical stimulation. Such a reconnection of the motor cortex to the spinal cord by means of the red nucleus has been observed only in rats that received a unilateral pyramidotomy at birth (38), an age at which the nervous system is known to be very plastic. The observed EMG recordings showed longer latencies than those in normal rats, suggesting reconnection to the spinal cord by means of a polysynaptic pathway. EMG activity in the proximal and medial muscles could be elicited in only 6 of 10 mAb IN-1-treated animals, but clear movements of trunk, shoulders, and biceps could generally be seen in all of the animals.

Several studies suggest a possible role of the rubrospinal tract in the cortical reconnection with the periphery. As already mentioned, the CST and RST share many functional similarities (39), and electrical stimulation experiments have shown that cortically evoked movements of the hand remain after pyramidotomy in the monkey (40) and the cat (41), although at higher current thresholds. To test the hypothesis of a compensatory takeover of CST function by the RST, we transiently inactivated both red nuclei by injecting the γ-aminobutyric acid agonist muscimol. Such injections result in a drug spread of 1.6 mm and a maximally reduced glucose uptake in a region of 1 mm around the injection site after 10 min, including, therefore, the entire red nucleus (42). At 30 min after injection, all ICMS-evoked peripheral responses were abolished, confirming a central role of the corticorubral pathway in this reconnection. In half of these animals, EMG activity could be reinduced 4 to 7 h after the muscimol injection. The recovery of the signal could not be achieved in all of the animals, probably because of homeostasis perturbations produced in the red nuclei by the muscimol injection.

In addition to this corticospinal reconnection by means of the red nucleus, physiological changes were also observed within the rubrospinal system. For the recorded medial muscles of the forelimb, a clear decrease in the stimulation threshold necessary to obtain EMG activity after red nucleus stimulation was observed in the lesioned, mAb IN-1-treated animals. Two mechanisms could be involved in these changes. First, it is possible that changes occur at the level of the red nucleus that make it more sensitive to stimulation. Such changes were shown to occur after a spinal cord injury (43), and were believed to be a consequence of a persistent decrease of synaptic inhibition at the level of the red nucleus. In our experiments, it is probable that the observed anatomical changes of the RST in the spinal cord contribute to the changes in both the excitability and the pattern of muscle excitation. Because of an increased number of collaterals emerging from the RST, stimulating the same number of RST fibers may lead to a stronger output at spinal cord level.

Taken together, the present observations demonstrate an unexpectedly high capability of the mature CNS to functionally reorganize after partial lesion and treatment with the mAb IN-1 which neutralizes the growth inhibitory protein Nogo-A.

The authors thank Mrs. Barbara Niederöst for providing the hybridoma cells and Mrs. Isabelle Weiss for discussions and critical reading of the manuscript. This work was supported by the Swiss National Science Foundation (Grants 31–45549.95 and 4038–043918.95), the International Research Institute of Paraplegia (Zurich), and the Christopher Reeve Paralysis Foundation (Spinal Cord Consortium, Springfield, NJ).

1. Little, J. W., Ditunno, J. F., Jr., Stiens, S. A. & Harris, R. M. (1999) *Arch. Phys. Med. Rehab.* **80,** 587–599.
2. Bishop, B. (1982) *Phys. Ther.* **62,** 1442–1451.
3. Basso, D. M., Beattie, M. S. & Bresnahan, J. C. (1996) *Exp. Neurol.* **139,** 244–256.
4. Noble, L. J. & Wrathall, J. R. (1989) *Exp. Neurol.* **103,** 34–40.
5. Kapfhammer, J. P. & Schwab, M. E. (1994) *J. Comp. Neurol.* **340,** 194–206.
6. Varga, Z. M., Schwab, M. E. & Nicholls, J. G. (1995) *Proc. Natl. Acad. Sci. USA* **92,** 10959–10963.
7. Chen, M. S., Huber, A. B., van der Haar, M. E., Frank, M., Schnell, L., Spillmann, A. A., Christ, F. & Schwab, M. E. (2000) *Nature (London)* **403,** 434–439.
8. Caroni, P. & Schwab, M. E. (1988) *J. Cell Biol.* **106,** 1281–1288.
9. McKerracher, L., David, S., Jackson, D. L., Kottis, V., Dunn, R. J. & Braun, P. E. (1994) *Neuron* **13,** 805–811.
10. Mukhopadhyay, G., Doherty, P., Walsh, F. S., Crocker, P. R. & Filbin, M. T. (1994) *Neuron* **13,** 757–767.
11. Pesheva, P., Spiess, E. & Schachner, M. (1989) *J. Cell Biol.* **109,** 1765–1778.
12. Snow, D. M., Lemmon, V., Carrino, D. A., Caplan, A. I. & Silver, J. (1990) *Exp. Neurol.* **109,** 111–130.
13. Asher, R. A., Morgenstern, D. A., Fidler, P. S., Adcock, K. H., Oohira, A., Braistead, J. E., Levine, J. M., Margolis, R. U., Rogers, J. H. & Fawcett, J. W. (2000) *J. Neurosci.* **20,** 2427–2438.
14. Caroni, P. & Schwab, M. E. (1988) *Neuron* **1,** 85–96.
15. Bandtlow, C. E., Schmidt, M. F., Hassinger, T. D., Schwab, M. E. & Kater, S. B. (1993) *Science* **259,** 80–83.
16. Schnell, L. & Schwab, M. E. (1990) *Nature (London)* **343,** 269–272.
17. Z'Graggen, W. J., Metz, G. A., Kartje, G. L., Thallmair, M. & Schwab, M. E. (1998) *J. Neurosci.* **18,** 4744–4757.
18. Thallmair, M., Metz, G. A., Z'Graggen, W. J., Raineteau, O., Kartje, G. L. & Schwab, M. E. (1998) *Nat. Neurosci.* **1,** 124–131.
19. Ghez, C. (1975) *Brain Res.* **98,** 93–308.
20. Hyland, B. (1998) *Behav. Brain Res.* **94,** 255–269.
21. Jarratt, H. & Hyland, B. (1999) *Neuroscience* **88,** 629–642.
22. Whishaw, I. Q., Gorny, B. & Sarna, J. (1998) *Behav. Brain Res.* **93,** 167–183.
23. Lawrence, D. G. & Kuypers, H. G. (1968) *Brain* **91,** 15–36.
24. Herzog, A. & Brosamle, C. (1997) *J. Neurosci. Methods* **72,** 57–63.
25. Neafsey, E. J., Bold, E. L., Haas, G., Hurley-Gius, K. M., Quirk, G., Sievert, C. F. & Terreberry, R. R. (1986) *Brain Res.* **396,** 77–96.
26. Whishaw, I. Q., Pellis, S. M., Gorny, B., Kolb, B. & Tetzlaff, W. (1993) *Behav. Brain Res.* **56,** 59–76.
27. Zagrebelsky, M., Buffo, A., Skerra, A., Schwab, M. E., Strata, P. & Rossi, F. (1998) *J. Neurosci.* **18,** 7912–7929.
28. Buffo, A., Zagrebelsky, M., Huber, A. B., Skerra, A., Schwab, M. E., Strata, P. & Rossi, F. (2000) *J. Neurosci.* **20,** 2275–2286.
29. Sato, M., Lopez-Mascaraque, L., Heffner, C. D. & O'Leary, D. D. (1994) *Neuron* **13,** 791–803.
30. Gallo, G. & Letourneau, P. C. (1998) *J. Neurosci.* **18,** 5403–5414.
31. Wang, K. H., Brose, K., Arnott, D., Kidd, T., Goodman, C. S., Henzel, W. & Tessier-Lavigne, M. (1999) *Cell* **96,** 771–784.
32. Kokaia, M., Ferencz, I., Leanza, G., Elmer, E., Metsis, M., Kokaia, Z., Wiley, R. G. & Lindvall, O. (1996) *Neuroscience* **70,** 313–327.
33. Fagan, A. M., Suhr, S. T., Lucidi-Phillipi, C. A., Peterson, D. A., Holtzman, D. M. & Gage, F. H. (1997) *J. Neurosci.* **17,** 2499–2511.
34. Scarisbrick, I. A., Isackson, P. J. & Windebank, A. J. (1999) *J. Neurosci.* **19,** 7757–7769.
35. Johnson, R. A., Okragly, A. J., Haak-Frendscho, M. & Mitchell, G. S. (2000) *J. Neurosci.* **20,** http://www.jneurosci.org/cgi/content/full/20/10/RC77.
36. Davies, H. E. & Edgley, S. A. (1994) *J. Physiol. (London)* **479,** 463–473.
37. Illert, M., Lundberg, A., Padel, Y. & Tanaka, R. (1978) *Exp. Brain Res.* **33,** 101–130.
38. Z'Graggen, W. J., Fouad, K., Raineteau, O., Metz, G. A., Schwab, M. E. & Kartje, G. L. (2000) *J. Neurosci.* **20,** 6561–6569.
39. Kennedy, P. R. (1990) *Trends Neurosci.* **13,** 474–479.
40. Lewis, R. & Brindley, G. S. (1965) *Brain* **88,** 397–406.
41. Hongo, T. & Jankowska, E. (1967) *Exp. Brain Res.* **3,** 117–134.
42. Martin, J. H. (1991) *Neurosci. Lett.* **127,** 160–164.
43. Chen, J. R. & Tseng, G. F. (1997) *Neuroscience* **79,** 449–462.